An Integrated Application of Neural Network and Markov Chain Techniques to Prediction of Lithofacies from Well Logs (Kansas Geological Survey Open File Report 2003-50)

G.C. Bohling and M.K. Dubois
Kansas Geological Survey
Lawrence, Kansas, USA

Abstract

The Permian Council Grove Group in the Panoma Field of southwest Kansas has yielded 80 x 10^9 meter^3 of gas from approximately 2600 wells from a 60-meter interval at depths of 800-1,000 meters since its discovery in the 1960's. Initial gas saturation, production rates and cumulative production in the Panoma Field are controlled by the distribution of porosity and permeability in the field, which are in turn controlled by the distribution of facies. We have used a single hidden-layer neural network to compute facies membership probabilities from geophysical well logs measured in approximately 470 wells throughout the field. The network was trained using facies assignments from detailed core descriptions in eight wells. For ease of use, the neural net prediction (feed-forward) code has been implemented as part of an Excel add-in using Visual Basic. However, the training of the network via backpropagation is too computationally intensive a task for this environment, and so is accomplished through an automated invocation of the neural network function provided as part of the public-domain R language. Code for the batch application of the trained neural network to log data from a large number of LAS (Log ASCII Standard) files is also implemented in the Excel add-in, providing an easy means for computing facies membership probabilities at a large number of wells. We then use public-domain Markov chain simulation code to produce a gridded realization of the facies architecture throughout the field, conditioned on the facies probabilities computed by the neural network. The simulation employs a transition probability model based on the facies sequences observed in core for the eight training wells, augmented by geological understanding of the expected facies relationships. This process provides an ideal means for merging geological knowledge with the dense quantitative information provided by geophysical well logs.

Introduction

In the Panoma Field, facies-controlled petrophysical properties dictate gas saturations and accurate discrimination of facies reduces error in predicted permeability and gas volume (Byrnes, Dubois, and Magnuson, 2001; Dubois and others, 2003). However, developing robust geologic models for reservoir analysis of large heterogeneous reservoirs like that in the Panoma Field is impractical by traditional methods. This study presents a possible solution to facies prediction using neural network and Markov chain techniques that will make possible the construction of a geologic and petrophysical model with sufficient detail to accurately represent the fine-scale vertical and lateral heterogeneities, a requirement for accurate reservoir modeling of the entire field.

Gas production in the Panoma Field is from seven, stacked fourth-order nonmarine-marine sequences in Council Grove Group (Permian, Wolfcampian) in the Hugoton Embayment of the Anadarko Basin (Fig. 1) deposited in a proximal, shallow position on a gently dipping ramp. Broad facies belts (Fig. 2) migrated in response to cyclical sea level fluctuations resulting a predictable vertical succession of facies within each sequence: 1) nonmarine redbeds, siltstone and fine sandstone or clay-rich siltstone and shale (Coastal Plain, two facies) deposited on an exposure surface (unconformity) on the underlying marine carbonate rock unit, 2) transgressive marine, shallow water carbonates with grain-supported textures (Shoal and Mound), 3) deeper water dark marine siltstones (Marine Siltstone and Shale) or silty carbonate mud- and wackestones (Normal Marine Carbonates), 4) agitated, shallow water packstones and grainstones (also categorized as Shoal and Mound) or quiet, shallow water dolomitized carbonate mudstones and peloidal wackestones (Tidal Flat and Lagoon) , and 5) tidal influenced, laminated and fenestral mudstones (also Tidal Flat and Lagoon). Subaerial exposure is evidenced by well-developed calcretes, root molds, and other weathering and pedogenic features. This categorization represents a combination of both lithofacies and depofacies designations.

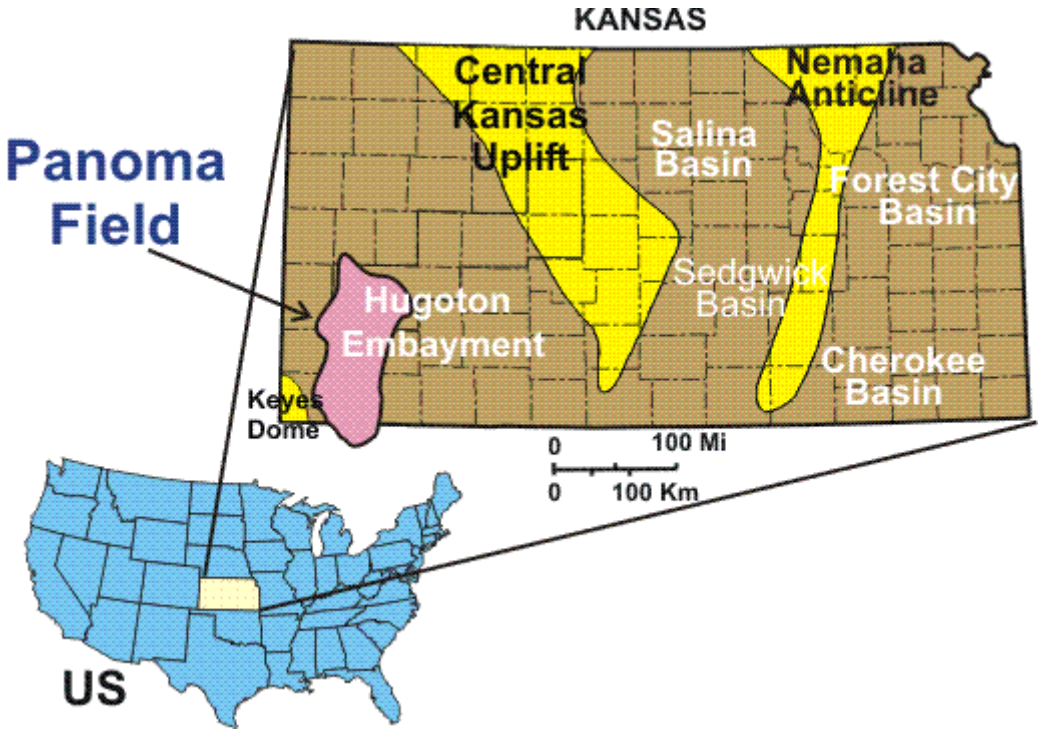

Figure 1. The Panoma Field is located in the Hugoton Embayment of the Anadarko Basin in southwest Kansas.

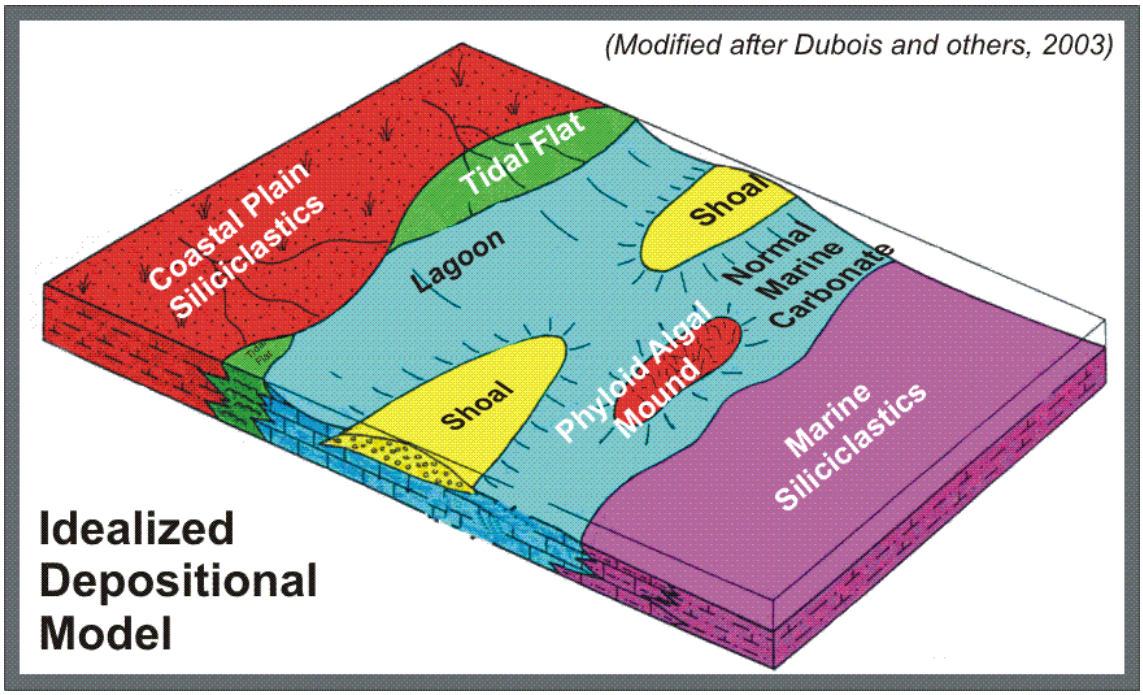

Figure 2. Idealized depositional model.

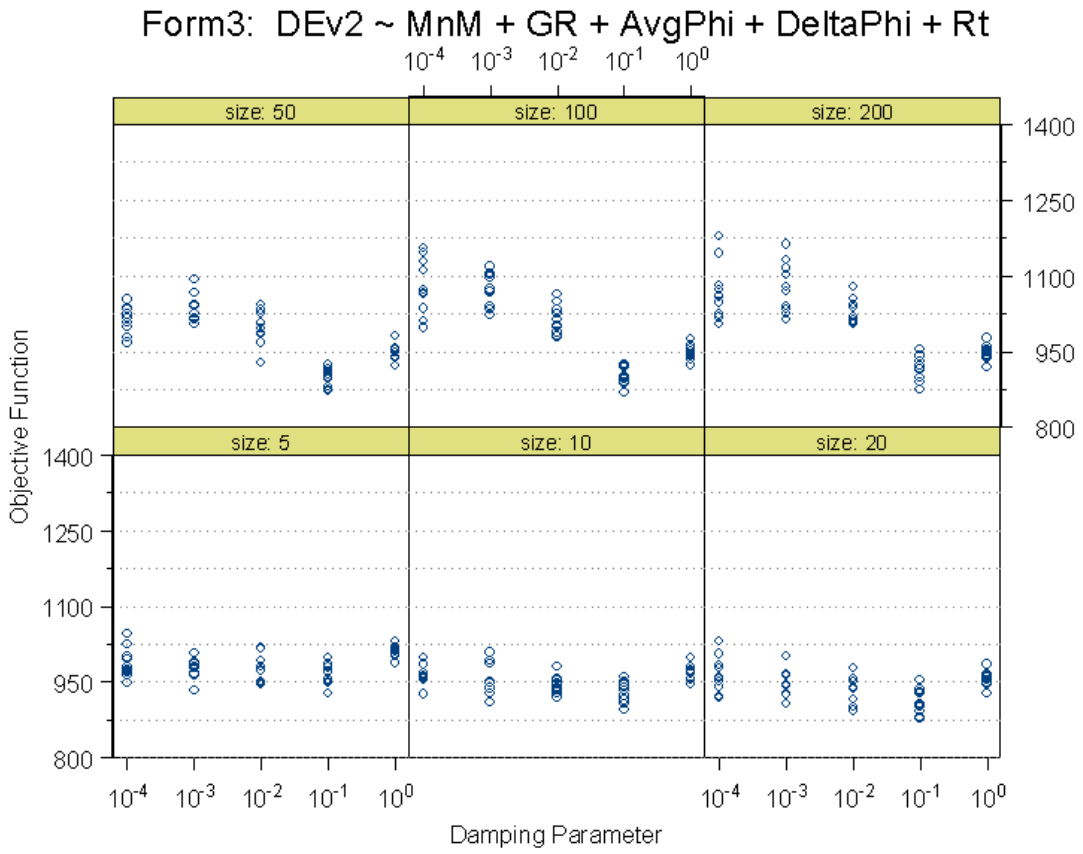

Figure 3. Cross-validation results for determination of optimal neural network model parameters (network size and damping parameter) for prediction of facies (DEv2) from specified logs.

Neural Net Predictions of Facies Probabilities

Based on the observed associations between geophysical well logs and facies designations from core in eight "keystone" wells distributed throughout the Panoma field, we have developed a neural network model for predicting facies from well logs. For this purpose we have used a standard single hidden-layer neural network (Duda, Hart, and Stork, 2001) with input-layer nodes corresponding to the selected geophysical well logs (plus a marine-nonmarine indicator curve generated from "tops" data in the well database) and output-layer nodes representing the set of facies membership probabilities. For ease of use, we have added Visual Basic code for neural network training and prediction to an existing Excel add-in for nonparametric regression and classification (Bohling and Doveton, 2000). However, the training routine invokes the public-domain "R" data-analysis system to perform the computationally-intensive optimization of network weights, using the *nnet* function developed by Venables and Ripley (1999). Both trial-and-error testing and automated cross-validation with keystone well data guided the prediction variable selection process. The final variables selected were marine/nonmarine indicator (MnM), gamma ray (GR), average (AvgPhi) and difference (DeltaPhi) of neutron and density porosity, deep resistivity (Rt), and photoelectric factor (PE) where available. We have focused our model calibration efforts on the selection of an appropriate number of hidden-layer nodes (network "size"), which governs the richness of the model, and an appropriate damping parameter, which constrains the magnitude of the network weights to help prevent overtraining. Cross-validation was automated using R (a.k.a. "S") language scripts. For each combination of network size and damping parameter, summary prediction statistics were computed for 10 different splits of the keystone well data into training (2/3) and prediction (1/3) subsets. Figure 3 shows the objective function values (a measure of the overall difference between "true" facies indicators and predicted probabilities) computed over the 10 prediction subsets for each combination of network size and damping parameter for the model without PE. Based on these and other results, we chose to use 50 hidden-layer nodes and a damping parameter of 0.1 for both models (with and without PE.)

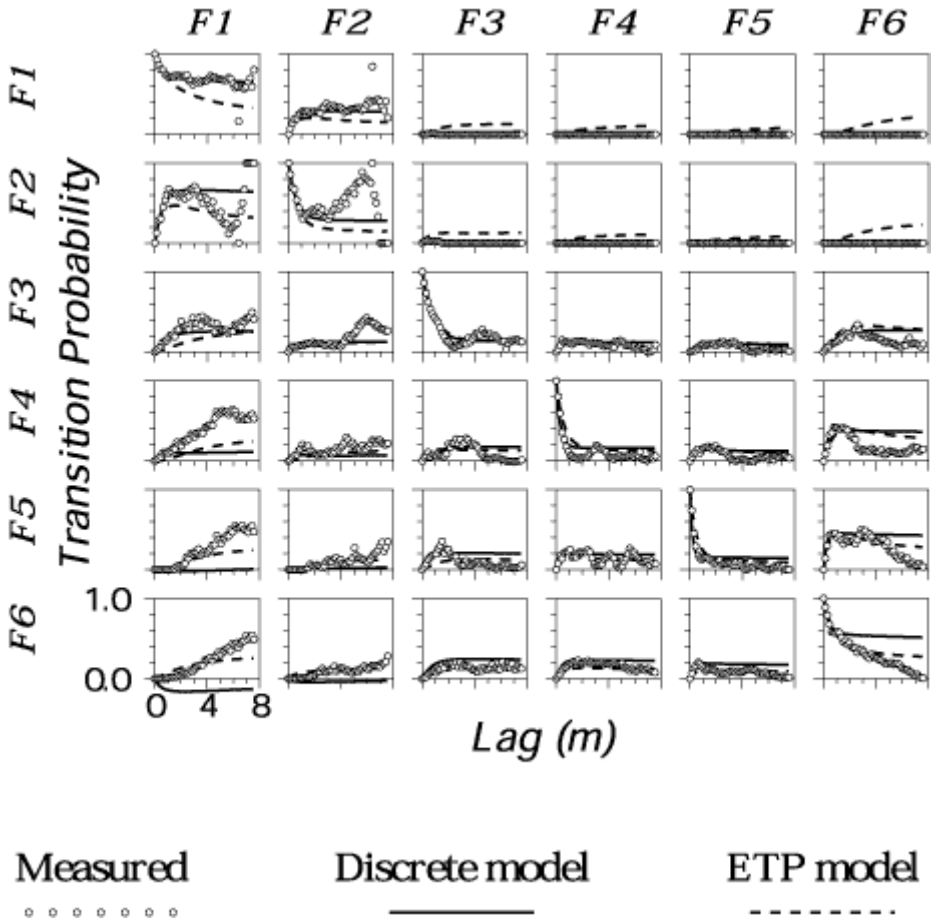

Figure 4. Vertical transition probabilities computed from core facies assignments together with discrete-lag and embedded transition probability models. The facies are: F1) coastal plain siltstone and sandstone, F2) coastal plain shale, F3) tidal flat and lagoon, F4) shoal and mound, F5) normal marine carbonate, and F6) marine siltstone and shale.

Transition probability modeling

The Markov chain simulation efforts so far have focused on the shallowest of the seven fourth-order sequences comprised of the Speiser Shale and Funston Limestone Formations, informally designated the A1 interval. For this work we have employed the T-PROGS modeling and simulation programs developed by Carle (1999). The Markov chain simulation employs a transition probability model representing the probability of occurrence of each facies at location (**x** + **h**) given the occurrence of a specified facies at location **x**, as a function of the lag vector **h**. As discussed in Carle and Fogg (1997), the development of a transition probability model from an observed facies sequence is similar in many ways to the development of an indicator covariogram model for that sequence. However, the transition probability approach allows more direct and intuitive incorporation of geological knowledge, including information regarding mean lengths of facies bodies in the principal coordinate directions. Figure 4 shows the transition probabilities versus vertical lag for the core facies in the A1 interval in the eight keystone wells together with two transition probability models, one derived from fitting to the empirical probability values at the fourth (0.6-meter) lag, and another derived from embedded transition probabilities and mean lengths computed from the same data. Embedded transition probabilities are computed by tallying transitions from one facies to another (ignoring "self-transitions"). Taking advantage of Walther's law, an embedded transition probability model derived from denser vertical data may be extended to lateral dimensions by changing the associated mean lengths in accordance with geological expectations. That is the approach used in this study. A transition probability model must obey a number of constraints in order to produce legitimate probability vectors at each lag. These constraints simplify inference somewhat but also contribute to discrepancies between empirical and modeled probabilities, as seen in Figure 4.

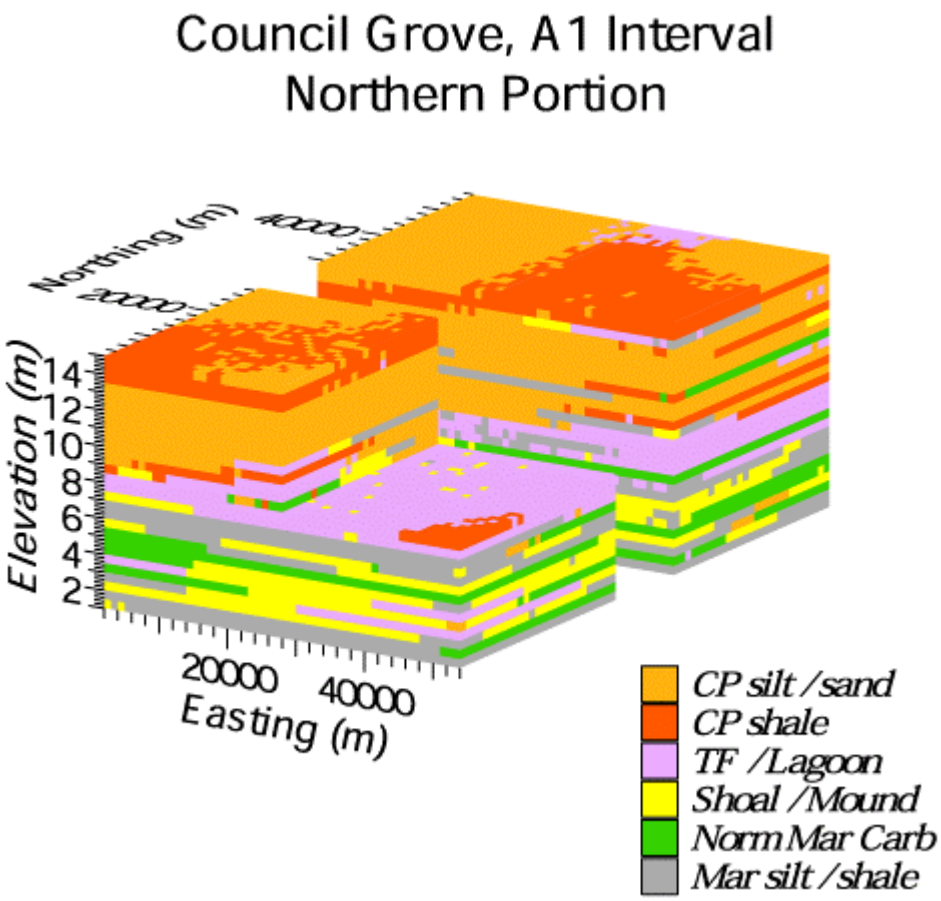

Figure 5. One realization of the Markov chain simulation for the A1 interval (Speiser Shale and Funston Limestone Formations) in the northern portion of the Panoma Field.

Markov chain simulation

Figure 5 shows a single Markov chain simulation of the facies distribution in the A1 interval in the northern portion of the Panoma Field, conditioned on facies occurrence probabilities predicted by the neural network. Batch application of the neural network model to well logs from 83 wells in this portion of the field produced facies occurrence probabilities at 8723 data points in this portion of the field, at a vertical spacing of 0.15 meters (0.5 feet). The model without the PE curve, representing a larger number of wells, was applied first. Then the model including PE was applied to those wells with a PE curve, overwriting the probabilities from the first model. The vertical coordinate employed in the model is actually a transformed "stratigraphic" elevation, adjusted to a nominal thickness of 16 meters (approximately the average thickness) at each location. There are 32 layers of cells in the vertical direction, each with a nominal thickness of 0.5 meters. The cells are 1000 meters long in each horizontal dimension, with 57 cells in the east-west direction and 58 north-south. Because the Markov simulation code accepts only one conditioning datum per grid cell, the probability vectors were "upscaled" from their initial vertical spacing (approximately three per grid cell) to a single probability vector for each cell intersecting a well. Since a set of facies membership probabilities can be regarded as a composition, the upscaled probability vector was computed as the closed geometric mean of the contributing probability vectors. Pawlowsky-Glahn and Egozcue (2002) suggest the closed geometric mean as the natural choice for representing the center of a set of compositional data.

The Markov simulation code generates an initial realization using sequential indicator simulation (based, in this case, on the transition probability model, rather than a covariogram model) and then performs several steps of simulated quenching (zero-temperature simulated annealing), updating facies assignments in order to more closely match the spatial structure dictated by the transition probability model while still honoring the conditioning data. However, although the T-PROGS code allows the option to condition on facies probabilities, as well as on "hard" facies indicators, as of this writing is not clear whether the code is in fact retaining and honoring the input probability vectors at the conditioning points during the

quenching steps. Instead, the code appears to sample from the input probabilities to seed the initial simulation, but then ignores these data during the quenching process. The quenching process could continue to honor the input probabilities by sampling from them at the conditioning nodes during the quenching process. We will investigate this issue further and modify the code as appropriate in ensuing work.

Conclusions

The Markov chain simulation technique provides a powerful means for fusing a conceptual geological model with quantitative information provided by subsurface measurements. In this study we are investigating the integration of facies probabilities derived from well logs using a neural network with a statistical representation of the facies architecture derived from detailed core investigations and a conceptual model of the associated depositional environments. A related study (Dubois and others, 2003) employed a sequential indicator simulation (SIS) based on indicator variograms to generate gridded realizations of the facies architecture from the neural network facies predictions at wells. Relative to this more traditional geostatistical approach, the transition probability modeling used in this study ". . . was developed to encourage infusion of subjective interpretation by simplifying the relationship between observable attributes and model parameters" (Carle, 1999, p. 5). In future work we will carry out more detailed comparisons of the SIS and Markov chain simulation techniques in order to evaluate the relative accuracy (or credibility) or their results as well as the relative ease of model development and inference for each approach.

References

Bohling, G.C., and Doveton, J.H., 2000, Kipling.xla: An Excel Add-in for Nonparametric Regression and Classification, Kansas Geological Survey, 69 p.

Byrnes, A.P., Dubois, M.K., and Magnuson, M., 2001, Western tight gas carbonates: comparison of Council Grove Group, Panoma Field, southwest Kansas, and western low permeability gas sands (abs.), 2001 American Association of Petroleum Geologists Annual Convention, v. 10, p. A31.

Carle, S.F., 1999, T-PROGS: Transition Probability Geostatistical Software, Version 2.1, Department of Land, Air and Water Resources, University of California-Davis.

Carle, S. F., and Fogg, G.E., 1997, Modeling spatial variability with one and multidimensional continuous-lag Markov chains, Mathematical Geology, v. 29, no. 7, p. 891-918.

Dubois, M.K., Byrnes, A.P., Bohling, G.C., Seals, S.C., and Doveton, J.H., 2003, Statistically-based lithofacies predictions for 3-D reservoir modeling: an example from the Panoma (Council Grove) Field, Hugoton Embayment, southwest Kansas, KGS Open-file Report 2003-30.
http://www.kgs.ku.edu/PRS/publication/2003/ofr2003-30/index.html

Duda, R. O., Hart, P. E., and Stork, D. G., 2001, Pattern Classification, Second Edition: John Wiley & Sons, Inc., New York, 654 pp.

Pawlowsky-Glahn, V., and Egozcue, J.J., 2002, BLU estimators and compositional data, Mathematical Geology, v. 34, no. 3, p. 259-274.

Venables, W. N., and Ripley, B. D., 1999, Modern Applied Statistics with S-Plus, Third Edition: Springer-Verlag New York, Inc., 501 pp.